Swiss Accelerator
Research and
Technology

CHART Collaboration

Phase 2 Intermediate Scientific Report

February, 2021

Introduction

This is the intermediate scientific report of CHART Phase-2 activities until the end of December 2020. It gives a summary of the goals and achievements of CHART over the 2019 – 2020 period. The projects were concentrated around the superconducting high-field magnets developments and beam-dynamics studies related to the FCC study at CERN.

The European Strategy for Particle Physics (ESPP) update has set a new target for the feasibility study of the FCC project within the time frame of the next ESPP update. The key-phrase of the strategy document states that "… Europe, together with its international partners, should investigate the technical and financial feasibility of a future hadron collider at CERN with a centre-of-mass energy of *at least 100 TeV and with an electron-positron Higgs and electroweak factory as a possible first stage*" [6].

The first period of CHART Phase-2 saw a significant growth in the number of projects carried out at the partner institutions. The majority of these aim at the FCC feasibility studies, for both the electron - positron collider FCC-ee and the hadron collider FCC-hh (see e.g. section 1.5). Some develop accelerator physics and technology areas of interest to other accelerator-driven scientific fields of research.

CHART can reach its full potential only as an active, distributed research network, embedded in an international web of partners. CHART Phase-2 projects mentioned in the following chapters have achieved significant progress towards this goal. Nevertheless, as can be seen in the summary of the CHART projects timelines at the end of this Introduction, some delays accumulated due to the slowdown in hiring under the present circumstances.

Superconducting magnets developments

The results of the ongoing CHART studies, as well as test results from the Canted Dipole 1 (CD1) and LBNL-built CCT magnets, will be presented at a technical review in 2021. Organized together with the FCC International Advisory Committee, it will also assess proposed magnet development strategy for the remainder of the CHART2 period and beyond (see detailed discussion in Chapter 1, section 1.5).

High field magnets component R&D is crucial at this early design and prototyping stage of high field magnet development and is pursued by several CHART participants.

As a continuation of the CHART Phase-1 activities, **MAGDEV1** project at PSI has established a high-field magnets development laboratory to continue the work on the design and prototyping of such magnets for FCC, investigating the options of employing both conventional and high-temperature superconductors. The CD1 demonstrator was completed and sent to our collaborators at the Lawrence Berkeley National Laboratory for tests of magnetic field performance at their cryogenic facility. Several BOnding eXperiment (BOX) samples are undergoing tests at the University of Twente in up to 11 T background field to investigate technological solutions to the channel-bonding problem in the Canted-Cosine_Theta (CCT) magnets.

The ETHZ led project **MAGRES** (Development of optimized resin systems for SC magnet coil production) is developing innovative epoxy solutions to optimize the cable performance under transverse stress. **MagAM** (Additive Manufacturing for Structural Components in Superconducting Coils), also at ETHZ, produces complex structures such as the winding formers of CCT coils or endspacers in cosine-theta coils, while adding enhanced functionality for increased adhesion, thus contributing to improved magnet performance.

Development and characterization of the Nb_3Sn wires that meet the FCC requirements take place at the University of Geneva. Developing methods for the fabrication of Nb_3Sn superconductors with enhanced current carrying capabilities that could be scaled to industrial production and by establishing the mechanical limits at which state-of-the-art and R&D Nb_3Sn superconductors can operate safely, to enable the development of magnets whose performance is close to the inherent limitation of the conductor.

High-Temperature Superconductors (HTS) have the potential to reach beyond the 16 T limit of the Nb_3Sn. In parallel to the FCC magnets and in order to gain experience with this material, CHART pursues a highly innovative **Bulk-HTS Undulator** project that has the potential to revolutionize the field of synchrotron light sources. Pursued in close collaboration with the Photonics Science Division of PSI, the project collaborates closely with the University of Cambridge and Fermi National Accelerator Laboratory in USA. Plans are to install the first prototype into the SLS2 light source at PSI.

FCC Beam Dynamics Studies

Beam stability aspects of the FCC collider design have been under study by the EPFL team. Simulations benchmarking utilized detailed analysis of the operational data from the LHC. Together with experiments performed on the running machine these studies resulted in significant contributions to the FCC Conceptual Design Report (CDR). In particular, the **Lumi-FCC-hh** project resulted in beam-beam interaction related luminosity measurements corrections relevant to the analysis of the LHC physics data analysis.

Machine learning techniques applied to the LHC data analysis were subject of investigations in the framework of a project performed in collaboration with the Swiss Data Science Centre (SDSC, located at EPFL and ETHZ).

FCC site feasibility related studies

Two CHART projects that were approved by the CHART Council in the Fall of 2020 address geology and geodesy aspects of the FCC tunnel. Development of a high-resolution 3D geological model and associated GIS-based subsurface data set for the FCC tunneling work are subject of the work performed at the University of Geneva (**FCC geological modeling** project).

FCC geodesy studies project at the ETHZ aims at the improvement of the geodetic reference systems and geodetic infrastructure already established for the current CERN site that will be required in order to cope with the demanding challenges of this large new infrastructure.

FCC-ee injector design

FCC-ee Injector Design and Test Stand at PSI is a multi-laboratory collaboration project, led by PSI and involving LAL (Orsay) and BINP (Novosibirsk). As part of the FCC-ee study the electron and positron linear accelerators of the injection chain will be designed and optimized including the electron gun(s), the positron production and capture systems, and the positron damping ring. An evaluation and optimization of the accelerator costs and the preparation of an advanced CDR are an integral part of this study.

For the positron production, a concept using superconducting magnet technology and high field RF capture cavities will be studied. A demonstrator using the SwissFEL 6 GeV linac as target driver will validate the concept.

High Field Magnet (HFM) development beyond CHART-2 (beyond 2025)

First deliberations for a European Accelerator R&D Roadmap on High Field Magnets, to be prepared by the Laboratory Directors Group (LDG), point to an R&D schedule for FCC-hh magnet system lasting three ESPP update periods (about 20 years). The current period is devoted to the establishment of research infrastructure, innovation in key technologies, and technology demonstration. The demonstrators would produce fields of the order of 12 T with adequate margins by 2025, with first 14-16 T demonstrators available by 2027. At the end of the period, key questions must be answered regarding the robustness and reach of the updated Nb3Sn. The second ESPP period would be devoted to a 16-T short-model program, where reproducibility and industrialization, as well as the preparation of infrastructure for long-magnet manufacturing and testing would be the main focus. Finally, the third ESPP period would focus on a long-magnet R&D and industrialization. Note that the above subdivision is indicative only, and that the individual R&D topics will almost certainly overlap.

In the light of the above, CHART2 covers the first part of the ongoing ESPP period. Its updated scope, therefore, includes an open yet focused canvassing study of novel technologies and designs, proof-of-concept subscale experiments, as well as the commissioning of infrastructure for the construction of up to 2-m-long magnets, and the production of first demonstrator coils. The CHART3 period must then focus on refined technology development and a fast-paced technology demonstration program, building and testing a series of accelerator magnets at the 12 T level and beyond. The CHART Roadmap for the period 2025 – 2028 will present and discuss the details (in preparation).

CHART projects approved by the Council: present status

CHART 2 Projects

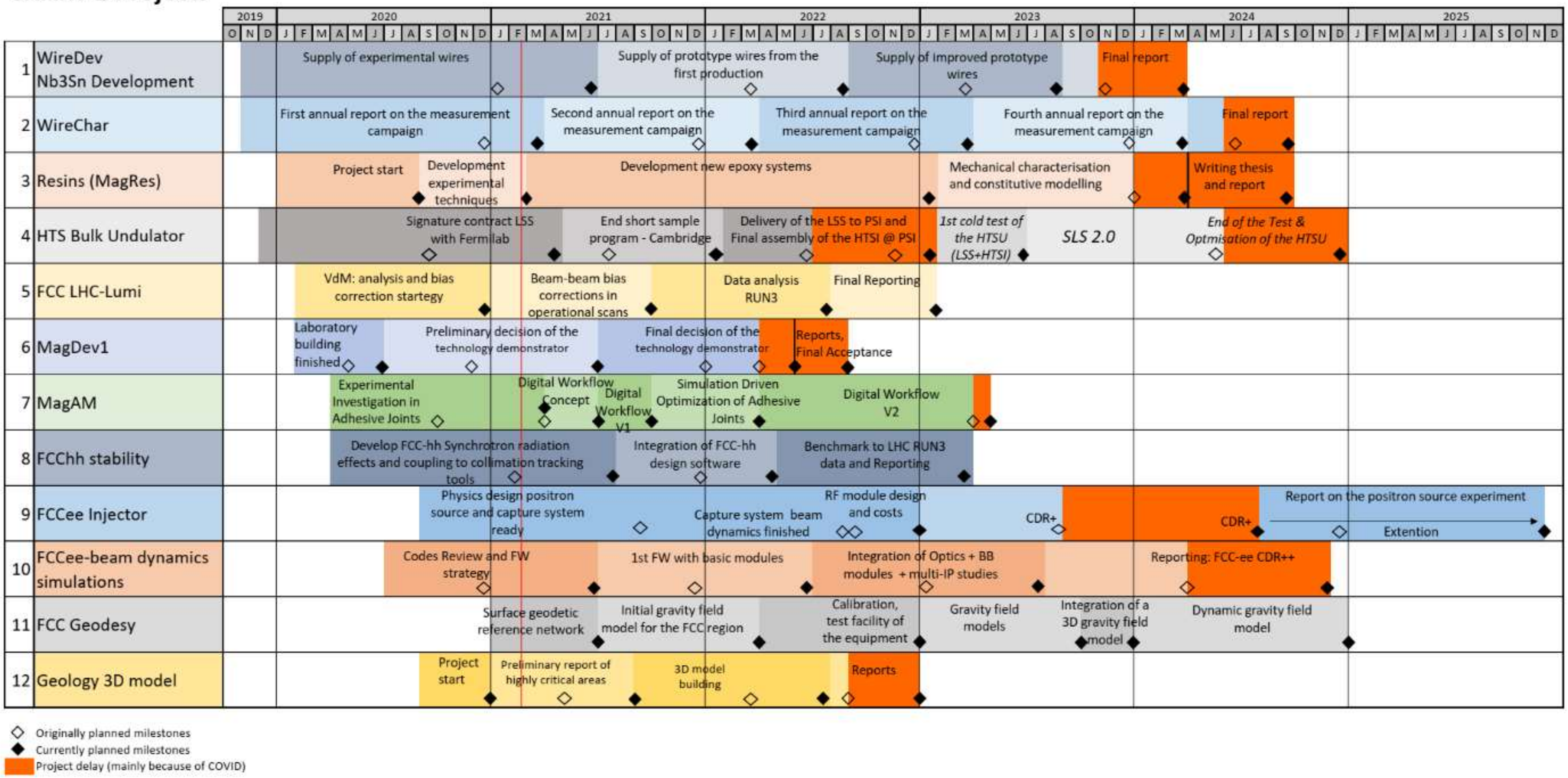

1. Report of MAGDEV1 project activities at PSI

Bernhard AUCHMANN, Michael DALY, Jiani GAO, Christoph HUG, Jaap KOSSE, Paul Scherrer Institut, Villigen, Switzerland

Over the reporting period, COVID-19 has caused several significant delays in the MagDev1 R&D program, due to the forced absence from the laboratory in March, April, and May 2020, but more importantly due to a delayed hiring process for MagDev1 engineers and technicians. More than half of the team has yet to arrive at PSI. Nonetheless we are glad to report below significant progress in all major areas.

1.1 Canted-Dipole 1 (CD1) Test and Take-Aways

Magnet R&D activities at PSI started during the CHART1 period and had as goals a) the creation of a conceptual design for a Nb_3Sn 16-T dipole magnet using the Canted-Cosine-Theta (CCT) technology, and b) the design, manufacturing and testing of a technology-model magnet. While the conceptual 16-T design was submitted and included in the FCC CDR [1] in 2018, the construction of the model magnet was finalized in October 2019 [2] i.e., in the first months of this reporting period; see Fig. 1.1. The magnet was shipped to LBNL, Berkeley, USA for testing in November 2019. An unfortunate delay of 2 months was incurred due to lost paperwork by the freight company (Lufthansa). As the magnet test was about to start end of March 2020, the COVID-19 crisis reached California, and the test had to be postponed until September 2020; see Fig. 1.1 bottom right. A first cool-down was followed by several powering ramps, of which at least one ended in a magnet quench when the magnet had reached 62.5% of maximal performance and produced 6 T of field in the bore. The initial powering of a magnet is almost always accompanied by a number of such "training quenches", and it is only after a full training campaign that a final judgement on the magnet performance can be made. Unfortunately, a problem in the helium-liquifying plant interrupted the test campaign. Currently it is foreseen to resume in January 2021.

Figure 1.1 Manufacturing steps of CD1: top left: coil winding; bottom left: magnet assembly; bottom middle: construction complete' bottom right: magnet ready for lowering into the test cryostat at LBNL. Top right: microscopic detail of LBNL's CCT5 magnet showing debonding of the impregnated coil from the channel wall (top and bottom right pictures courtesy of Diego Arbelaez, LBNL).

From the past years of design and construction, from the initial powering, and from two tests of CCT magnets produced in Berkeley over the past two years, we have reached some preliminary conclusions: 1) PSI has built a Nb_3Sn magnet that can be powered and produces high magnetic fields. This statement is non-trivial, since the brittle Nb_3Sn material has caused numerous coils to fail in various R&D programs worldwide. 2) CCT magnets produced by LBNL have so far shown consistently poor training performance, i.e., they needed too many training quenches to reach their full potential. There is now direct evidence from microscopic analyses that debonding between the epoxy-impregnated cable and the channel walls of the winding mandrels is an important factor in the limited CCT performance; see Fig. 1.1 top right.

We fully expect the CD1 magnet to suffer from a similar bond limitation and view the weakness of the adhesive bond as a fundamental limitation of today's CCT technology. At the same time, we acknowledge that adhesive bonding failures by no means only exist in CCT-type magnets. More classical magnet types such as cosine-theta coils have shown performance limitations due to de-bonding in the glued magnet ends. However, the shear amount of adhesive bonds in every location along the cable of a CCT magnet makes this failure mechanism particularly harmful.

In the course of a PhD thesis by Jiani Gao, defended successfully in August 2020 at EPFL [3], magnet-protection for CCT-type magnets has been studied. The main results of the thesis are a first-of-a-kind 2D simulation of a fast-oscillating discharge (CLIQ – coupling-loss-induced-quench) [4], and a subscale experiment, studying the potential of current-based quench detection by means of a co-wound superconducting sensing wires [5]. Ms. Gao's modeling work predicts that CCT magnets are well-protectable in a particle accelerator. A validation of the models in the CD1 test campaign will conclude the protection study. As for the subscale detection experiment, follow-up studies will build on the experience from the Jiani's experimental work.

1.2 The BOX Program

Given the bonding-failure that plagues CCT magnets as well as other magnet types, it has been decided to devote a fast-turnaround R&D program to precisely this issue. The so-called BOX samples (BOnding eXperiment) are designed to reproduce the shear forces experienced by the impregnated cable in the CCT winding former in a small sample that can be powered in the field of a background solenoid; see Fig. 1.2. For the test setup, a collaboration with TU Twente, the Netherlands, was set up. MagDev1's Michael Daly leads the design and construction of the BOX samples. BOXs 1 and 2 were built as to represent as closely as possible the CD1 configuration. The idea was that training of these two samples in the background-field solenoid would constitute a baseline upon which the R&D program must improve substantially. Solutions that work on BOX samples would then be implemented on CCT magnets in the hope to overcome their current limitation.

BOXs 1 and 2 were tested in September 2020 and showed clear training behavior with about 40 quenches per sample recorded. Post-test analyses with dye penetrant have shown clear indications of cracking and de-bonding on the BOXs channel walls. Acoustic signals showed characteristics similar to those recorded on full-scale CCT magnets. Advanced tomographic imaging is currently under way. Following this initial success, four more BOX samples have been manufactured and shipped to Twente for testing, which is scheduled for before and after the 2020 Christmas break.

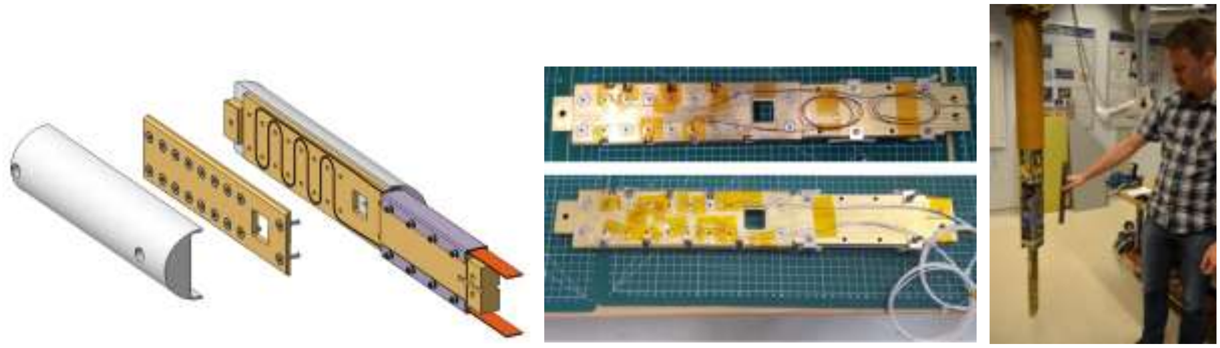

Figure 1.1 BOX samples: left: schematic view of assembled BOX sample; middle: BOX1 (top) and BOX 2(bottom); right: BOX1 mounted on the TU Twente superconducting transformer prior to cool-down (photo courtesy of S. Otten and A. Kario, TU Twente).

With only 1 m of cable, the material cost per sample is negligible. Sample construction of the last four samples took two weeks per sample on average. The cold powering test costs about CHF 5kCHF. These numbers underline the potential of the BOX sample as an R&D tool, when compared to development times of 1-2 years for a full-scale magnet, 350 kCHF material cost, and about 140 kCHF per magnet test. Numerous daring ideas can be tried out with relatively little risk. Among the ideas on the R&D plan are: no-impregnation samples, wax impregnation samples, ceramically coated formers and bare-cable windings, high-viscosity filled-epoxy systems with vacuum-pressure impregnation, metal impregnation, mullite-Ti-O_2 braid insulation, glass-paste impregnation, and many others more. This program constitutes by far the fastest-turnaround setup for studying the training-quench phenomenon that has been devised to date. Collaborations for BOX samples have been launched with material scientists at PSI, TU Twente, LBNL, and CERN.

1.3 HTS NI-Coil R&D

Non-insulated (NI), solder impregnated HTS coils wound from Rare-Earth-Bismuth-Copper-Oxide (REBCO) tape (NI coils) have proven impressive shear robustness. The technology is applicable for coils of moderate size and inductance, that are powered in DC mode. One such application is a high-field superbend magnet for the Swiss Light Source. Another potential application is the flux concentrator magnet around a target of a positron source, to be installed at SwissFEL in the course of a CHART2 FCC-ee Injector project.

Tokamak Energy Ltd in the UK is a compact-fusion startup company that has established itself over the past five years as a leader in NI-coil technology. For MagDev1 to deliver meaningful progress in a new field in a rather short time, we have forged a collaboration with Tokamak Energy (TE), wherein TE licenses their NI-coil technology to PSI while PSI shares any improvements in coil technology and mechanical aspects back with TE. A "heads of agreement" document has been iterated and agreed upon by both partners, and the licensing agreement is currently being drafted. At the same time, and in anticipation of the final agreement, an HTS coil-winding setup has been built at PSI in collaboration with CERN and is currently being commissioned. A young engineer, Dr. Jaap Kosse, has started to work on the project in October 2020 and has made good progress in literature analysis, numerical multi-physics modeling, and commissioning of the winding setup.

1.4 The MagDev Laboratory

The CD1 magnet was built in a 90 m^2 room on the east side of PSI, which has proven exactly the right size to build this one magnet. Neither could a larger magnet have been built there, nor could more than one project have proceeded simultaneously. For this reason, a new laboratory space was specified that would allow three teams to progress on independent projects, including up to 2-m-long magnets, and improve all aspects of magnet development: the coil winding, heat-treatment, impregnation, mechanical assembly, and metrology. A 400 m^2 extension to the WLHA building was constructed in the first half of 2020 (see Fig. 1.3 left). In July 2020, the MagDev lab moved from the east side to the new facility. The reaction furnace was recommissioned in September 2020 and the reaction diagnostics improved by the addition of a highly sensitive oxygen sensor. The HTS winding setup is being commissioned (see Fig. 1.3 right), while an LTS winding table for up to 2-m-long coils is in the conceptual-design phase. A tubular furnace was specified and procured and is due to arrive before the end of the year. This furnace will allow to operate at temperatures of up to 1300ºC in vacuum, argon, or with a 2-gas mixture (whereas the large existing furnace can operate only below 700ºC in argon). New safety equipment was introduced for work with chemicals (ventilated workspace, ventilated storage). The specification process has started for an autoclave for vacuum-pressure impregnation of up to 2-m-long coils. A 3-D scanning metrology system was acquired that will allow the team to perform unprecedented quality-control throughout the coil- and magnet-manufacturing processes. Special care was taken in all acquisitions to follow the rules of PSI's purchasing regulations, and to create a magnet-development facility that can flexibly adapt with changing projects phases, team configurations, and technologies.

Figure 1.2 Left: The area up to the yellow pallet racks constitutes the new MagDev Laboratory at PSI. Right: Tensioning system of the HTS winding setup.

1.5 Other Developments and Next Steps

The European Strategy for Particle Physics update has arrived and has set a new technical target and time frame for the FCC-hh magnet development. The key-phrase of the strategy document states that "… Europe, together with its international partners, should investigate the technical and financial feasibility of a future hadron collider at CERN with a centre-of-mass energy of *at least 100 TeV and with an electron-positron Higgs and electroweak factory as a possible first stage*." [6]

In this light, the target of Nb_3Sn LTS R&D is firmly on 16 T magnets and will not be lowered at least before a future strategy update. With an e+e- collider first, the timeline for FCC-hh is extended. The present strategy period of 5-7 years will be dedicated to meticulous component R&D, i.e., a thorough understanding of materials, manufacturing processes, and innovative design options such as low-prestress compact-coil designs, and stress-management coils (see below). The new developments must be proven first in an agile program in the 12-T range, which will be followed over the next strategy period by a short-model program for 16-T magnets, and a preparation of facilities for long-magnet R&D. Overall, the pre-industrialization phase of magnet R&D for FCC-hh, in this roadmap, will last for more than 20 years.

For HTS options, the "… at least 100 TeV …" formulation in the European Strategy for Particle Physics paper is expected to lead to a renewed push for 20 T accelerator magnets. Most likely, such field levels will first be achievable in an LTS-outsert / HTS-insert configuration. We note that the above NI-coil technology is not applicable for large-scale accelerator magnets that need to be ramped with the beam energy. While MagDev1's work on NI coils will produce deliverables with direct impact for the PSI accelerator facilities and introduce HTS technology at PSI, this endeavor shall be followed by an R&D in line with the ESPP goals.

Another consequential document that has been published recently is the US-MDP (Magnet Development Program) roadmap for the coming five years [7]. Over the past years, LBNL has had limited success in the CCT program, and made significant progress in HTS coil development. At the same time, FNAL built a 4-layer cosine theta magnet that achieved a world-record 14.5 T on-axis with extensive training, but strongly deteriorated performance after the first thermal cycle. For the coming US-MDP R&D period, the Nb_3Sn magnet R&D goal is to explore the potential of stress-management concepts. While LBNL will continue their CCT development, FNAL will focus on SMCT (Stress Managed Cosine Theta) coils, whereby coil blocks of a cosine-theta coil are wound into slots of a winding former, which is reacted and impregnated with the coil. From our own experience, we judge that while SMCT resolves some of the CCT's obvious challenges when it comes to the construction and assembly of 15-m-long magnets, it risks to not only replicate but aggravate the bonding-related performance problems.

Therefore, we note that

1. stress-management ideas are now studied by the two leading magnet-development laboratories in the US
2. the bonding thematic, that we address through the BOX program (see above), constitutes a critical impediment to performance of stress-managed magnets; it is also relevant for other magnet types
3. CHART MagDev continues to support R&D on stress-management solutions, in particular through the BOX program; at the same time, we critically re-assess the relative advantages, risks, and disadvantages of the CCT design for FCC-hh.

Beyond the bonding issue, we see difficulties in the CCT design with the assembly process of 15-m-long coils, the industrialization of coil winding, the cost of the winding former, and in the tight geometrical tolerances on conductor positioning. As briefly mentioned above, an alternative way to evade the forbidding mechanical stresses in high pre-stress compact coils (today's cosine theta or block coils) may be to pursue a low pre-stress compact-coil approach. This approach has not been studied for impregnated Nb3Sn coils by any laboratory to date. The results of the ongoing studies, as well as test results from CD1 and LBNL-built CCT magnets, will be presented at a technical review in 2021, where we shall propose a strategy for the remainder of the CHART2 period and beyond. In the meantime, we strive to prepare the laboratory facilities for the construction of up to 2-m-long Nb3Sn coils, not necessarily of CCT type.

Given all of the above, as of January 2021 MagDev1 started additional R&D activities with two new collaborators: 1) André Brem, a post-doc who has worked on CHART1 resin R&D at ETHZ before, will join the PSI MagDev1 team to intensify work on the material- and process engineering of the coil composite, and 2) Giorgio Vallone, a CERN- and LBNL-trained engineer, studies novel low-prestress mechanical concepts for compact coils such as cosine-theta and block-coil types. In addition, we start a collaboration with Fachhochschule Nordwestschweiz, Department of Controls and Automation, on the digitization of manufacturing and quality control processes, which is a crucial asset for reproducible and reliable coil manufacturing

[1] M. Benedikt et al. Future Circular Collider Study. Volumes 1,2,3: Conceptual Design Report, preprint edited by CERN accelerator reports, CERN-ACC-2018-0058, Geneva, December 2018. Published in Eur. Phys. J. ST.

[2] G. Montenero, B. Auchmann, D. Arbelaez, L. Brouwer, S. Caspi, R. Felder, F. Lackner, S. Sanfilippo, S. Sidorov, D. Smekens, J. H. Swanson. Coil Manufacturing Process of the First 1-m-Long Canted– Cosine–Theta (CCT) Model Magnet at PSI, IEEE Trans. on Appl. SC. 29(5), 2019.

[3] J. Gao, Analysis of Quench Detection and Protection of a Nb3Sn CCT Technology Demonstrator Dipole for FCC, PhD Thesis, EPFL, 2020.

[4] J. Gao, B. Auchmann, L. Brouwer, A. Pautz, S. Sanfilippo. Modeling of Quench Protection Concepts for Canted-Cosine-Theta Type High- Field Magnets, IEEE Trans. on Appl. SC. 30(4), 2020.

[5] J. Gao, B. Auchmann, A. Pautz, S. Sanfilippo, Current-based quench detection test via a co-wound superconducting sensing wire, submitted to IEEE Trans. on Appl. SC, 2020.

[6] European Strategy Group, 2020 Update of the European Strategy for Particle Physics, June 2020.

[7] S. Prestemon, K. Amm, L. Cooley, et al. The 2020 Updated Roadmaps for the US Magnet Development Program, preprint, November 2020.

2. Report of the s.c. wire development activities at UNIGE

Tommaso BAGNI, Gianmarco BOVONE, Florin BUTA, Carmine SENATORE
DQMP, University of Geneva, Geneva, Switzerland

Amalia BALLARINO, Bernardo BORDINI, Jose FERRADAS TROITINO, Simon C. HOPKINS
CERN, Geneva, Switzerland

High performance Nb_3Sn wires represent a crucial element for the development of high-field accelerator magnets capable of providing 16-T dipolar fields. From a first analysis of the main magnet design parameters, a 16-T field in a dipole configuration translates into a requirement of a minimum non-Cu J_c of more than 1'500 A/mm^2 in the superconductor at 16 T and 4.2 K [1] (non-Cu J_c corresponds to the critical current divided by the wire cross-section area minus the Cu area). This target is approximately 25% higher than the best commercial wires and the gap becomes even larger if the reduction of the critical current due to the electromagnetic forces during operation is taken into account. The experience gained with the development of the 11 T dipoles for HL-LHC shows that severe damages to the superconductor performance occur at stress levels of ~150 MPa. On the other hand, it appears clear from various conceptual studies that the design of a 16-T dipole entails peak stresses in the 200 MPa range. An equally important objective of the conductor R&D needs thus to be the development of strategies for the enhancement of the mechanical stress tolerance of Nb_3Sn wires, based on a better understanding of the mechanisms behind the permanent degradation of the critical current.

In the frame of two research agreements under the umbrella of CHART2, UNIGE and CERN collaborate with the scope of

1) developing methods for the fabrication of Nb_3Sn superconductors with enhanced current carrying capabilities that could be scaled to industrial production;

2) establishing the mechanical limits at which state-of-the-art and R&D Nb_3Sn superconductors can operate safely, to enable the development of magnets whose performance is close to the inherent limitation of the conductor.

2.1 Advanced Niobium-Tin superconductors for next generation particle colliders

Pushing Nb_3Sn technology towards its ultimate performance requires research work extending from fundamental aspects to material engineering and applied science. The in-field critical current capabilities for any type-II superconductor rely on its ability to impede vortex motion, i.e. to pin the vortex lines into the material. This ability is given by the presence of the so-called pinning centers, features in the material that interact attractively with individual vortices. Grain boundaries represent the primary pinning centers in Nb_3Sn: higher current densities are thus obtained in materials that have finer grains. In present-day high-performance wires, Nb_3Sn has average grain sizes of typically 100-200 nm [2,3]. In the period covered by this report, we worked to the development of methods for refining the grain size of Nb_3Sn with processes scalable to the industrial production of wires. The inhibition of the grain growth in the presence of oxide nanoparticles and, in particular, the so-called internal oxidation method [4] appear to be the most promising avenues. The key ingredient for the internal oxidation is the use as a precursor of Nb-alloys containing a small percentage of Zr. The composite wires prepared at UNIGE have an external Sn configuration, in which a Nb-alloy filament, 0.22 mm in diameter, is surrounded by successive electrodeposited layers of Cu, Sn and Cu. In the center of the Nb-alloy, a compacted core of metal oxide powder serves as the oxygen source for the internal oxidation of Zr: during the heat treatment the metal oxide powder is reduced and oxygen diffuses into the Nb-alloy where it oxidizes the highly reactive Zr. For this to work, the Gibbs free energy of formation of the metal oxide that acts as an oxygen source needs to be higher than those of ZrO_2. As a result, very fine particles of ZrO_2 are formed that inhibit the growth of the Nb_3Sn during the reaction of Nb with Sn. Multiple combinations of different Nb-alloys and oxygen sources were studied, in an attempt to further improve the high magnetic field properties and identify materials that may be of interest for the development of multifilamentary wire. In particular, custom Nb-alloys containing Zr and Ta were produced and tested to combine the increase in the critical current density due to the reduced grain growth with high upper critical fields due to the presence of Ta, which is a well-known dopant for increasing B_{c2}. The main properties of selected wires are summarized in Table I.

Table I. Main parameters and properties of the Nb_3Sn wires

Filament material (wt%)	Metal oxide powder	Average grain size, short axis (nm)	Average grain size, long axis (nm)	T_c (99%) (K)	B_{c2} (99% R_n) (T)
Nb-7.5Ta (ref.)	-	92	118	18.2±0.1	27.9
Nb-1Zr	SnO_2	57	95	17.7±0.1	26.7±0.1
Nb-1Zr	CuO	51	90	17.8	27.0±0.1
Nb-7.5Ta-1Zr	SnO_2	60	87	18.0±0.2	28.7±0.2
Nb-7.5Ta-2Zr	SnO_2	55	95	18.1	29.2±0.2

As revealed by the imaged fracture surfaces reported in the left panel of Fig. 2.1, the internal oxidation of Zr led to a finer grain structure. The Nb_3Sn grains are not equiaxed but slightly elongated, with an aspect ratio of 1.5-1.7. Measures of the Nb_3Sn grain size in these materials, reported in Table I, confirm the visual evaluation: grains are substantially smaller in samples based on internally oxidized Nb-Zr-alloys than in the reference samples based on Nb-7.5Ta without added oxygen, the lowest average grain sizes being close to 50 nm. The refinement appears slightly more pronounced in the short axis direction, with a ratio of around 0.6 between the respective lengths in the internally oxidized and the Nb-7.5Ta-based samples as compared to 0.7-0.8 in the long axis direction.

The critical current densities follow the trend expected based on the refinement of the grain structure. As determined from inductive measurements, the layer J_c (i.e. the critical current divided by the area of the superconducting layer) of the samples based on Nb-alloys with internally oxidized Zr are superior to those based on Nb-7.5Ta. The samples prepared with Nb-7.5Ta-1Zr and Nb-7.5Ta-2Zr showed the highest critical current densities at high magnetic fields (above 12 T based on extrapolation of measurements below 7 T), as shown in the right panel of Fig. 2.1. The extrapolated layer J_c at 16 T and 4.2 K of the samples containing internally oxidized Zr exceeds 3'000 A/mm^2, a result significantly above the 2'000 A/mm^2 measured in the best high performance inustrial wires.

A very important result of this work is that it shows convincingly that Nb_3Sn based on the Nb-7.5Ta-1Zr and Nb-7.5Ta-2Zr alloys have upper critical fields that are significantly higher than those based on Nb-7.5Ta, an alloy that otherwise was optimized as a filament material leading to a high upper critical field. Upper critical fields as a function of temperature were obtained from resistive measurements in magnetic fields of up to 33 T at the European High Magnetic Field Laboratory in Grenoble, France. To our best knowledge, the B_{c2} values we determined on these samples are the highest ever measured at 4.2 K on doped Nb_3Sn, with a record value of 29.2 T at 4.2 K measured on the wire prepared with the Nb-7.5Ta-2Zr alloy [5]. Further experimental work is needed to understand how the co-doping with Zr and Ta leads to higher critical fields, however we can speculate that further enhancements may be possible.

The transfer of the present results to prototype multifilamentary wire is ongoing.

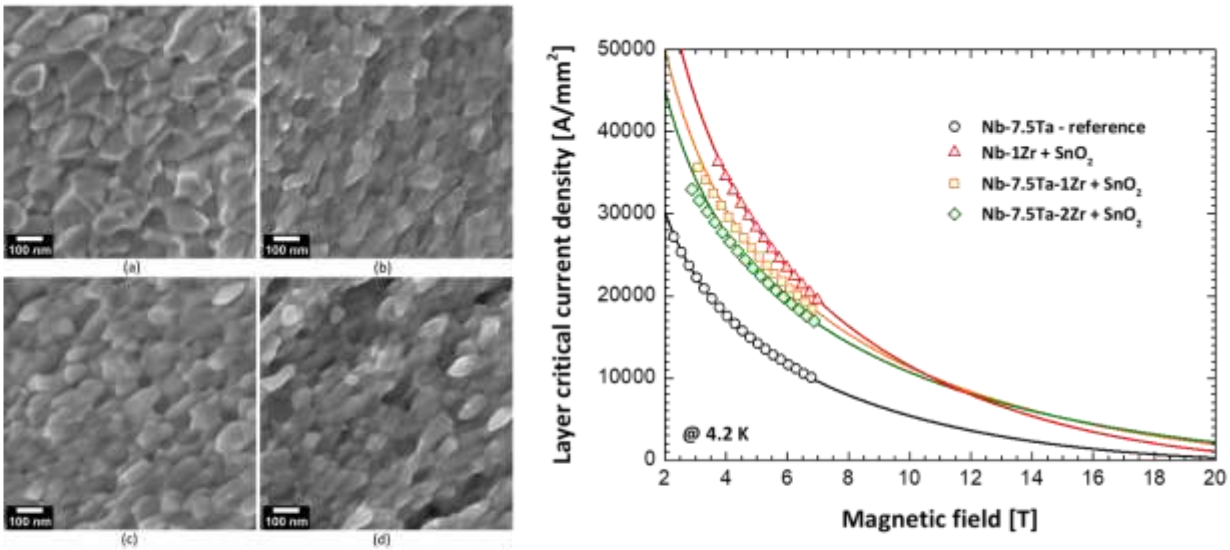

Figure 2.1 (Left) SEM images of Nb_3Sn grains at fractured surfaces from samples based on (a) Nb-7.5Ta (reference), (b) Nb-1Zr+SnO_2, (c) Nb-7.5Ta-1Zr+SnO_2 and (d) Nb-7.5Ta-2Zr+SnO_2. The refinement of the grain size in the samples containing Zr is evident. (Right) Enhancement of the critical current densities (at 4.2 K) of samples based on Nb-Zr and Nb-Ta-Zr alloys with an oxygen source compared to reference samples based on Nb-7.5Ta without an oxygen source.

2.2 Multiphysics properties of advanced superconductors

Nb_3Sn accelerator magnets' coils are wound using insulated Rutherford cables composed of many single wires transposed together. These cables are ultimately resin-impregnated, forming a solid winding pack intended for a homogeneous distribution of the mechanical loads inside the coils. Typically, the stress on the conductor at the nominal field is compressive in the transverse direction and localized at the magnet midplane. Assessing the stress tolerance of Nb_3Sn Rutherford cables becomes therefore essential to estimate the transport current properties of the conductor within the magnet. However, experiments with full-size cables under transverse compressive stress are difficult to conduct and are possible only in very few facilities around the world. At the University of Geneva, we have developed special probes that allow extracting from a single-wire experiment quantitative information about the degradation of a Rutherford cable under transverse stress [6]. In the period covered by this report, we have performed a measurement campaign to investigate the stress dependence and the irreversible reduction of the critical current under compressive transverse load in state-of-the-art Nb_3Sn wires produced by Powder-In-Tube (PIT) method and Restacked-Rod-Process (RRP) [6,7]. Tests were performed on single wires that were resin impregnated similarly to the wires in the Rutherford cables of accelerator magnets. The main results were the following:

i) The irreversible stress limit, σ_{irr}, of the wires was defined as the transverse stress value leading to a permanent reduction in the critical current of 5%, with the convention of performing the measurement at B = 19 T on samples impregnated with epoxy-L resin. An example is shown in the left panel of Fig. 2.2. The PIT wires tested during this measurement campaign have 192 filaments and two different diameters, 1.00 and 0.85 mm. Both were developed by Bruker EAS for CERN: the one at 1.00 mm for the FRESCA2 dipole and the one at 0.85 mm for the MQXF quadrupoles of HL-LHC. The RRP wires, produced by Bruker OST, are composed of 108 sub-elements embedded in a Cu matrix following the 108/127 hexagonal restack and have two different diameters, 0.85 mm and 0.7 mm. Samples were extracted from production billets used for the MQXF quadrupoles (Ø = 0.85 mm) and for the 11 T dipoles (Ø = 0.7 mm) of HL-LHC. The PIT wires reached their irreversible limit at σ_{irr} = 110 MPa, which is a rather low value. The irreversible stress limit for RRP wires has been found to be in the range of 145 – 175 MPa. We identified a remarkable effect of the initial axial strain state in the wire's response to transverse loads, which is behind the range of values measured for σ_{irr} [7].

ii) The irreversible stress limit was found to be largely controlled by the rigidity of the impregnation resin. In our tests, we measured an increase of σ_{irr} of about 50 MPa by replacing the relatively soft epoxy-L impregnation with Stycast or by adding a glass-fiber reinforcement [6]. It is envisaged to test the effects on σ_{irr} of novel impregnation schemes developed in the cooperation between PSI and the ETHZ Soft-Materials Lab.

iii) Two phenomena work together to determine the irreversible reduction of the wire performance: mechanical fracture of the superconducting filaments and plastic deformations of the copper matrix. First, Nb_3Sn is a brittle intermetallic compound characterized by a strong propensity to fracture. Second, the superconducting filaments of a Nb_3Sn wire are embedded in a soft Cu matrix; hence it is relatively easy to deform plastically. Plastic deformation of the stabilizing matrix due to an external load leaves the Nb_3Sn filaments under residual stress after unloading. By studying the wires' response at different magnetic fields after load removal, we concluded that the dominating effect behind critical current degradation in PIT and RRP wires is different: it is the residual plastic strain in the Cu matrix for the PIT wires and the formation of cracks in the superconductor for the RRP wires.

As a complement to the electro-mechanical tests, we have also performed synchrotron tomography experiments to study the internal features of Nb_3Sn wires and get insights into the mechanisms behind the permanent degradation of the critical current [8]. In particular, it is known that the presence of voids in the superconducting filament structure, which are formed mostly during the activation heat treatment, determines localized stress concentrations and possibly the formation of cracks. Our analysis tool is the combination of micro-tomographies with an unsupervised machine learning algorithm, which is able to autonomously isolate, reconstruct and analyze the voids (right panel of Fig. 2.2). We were capable to completely characterize the voids present in five different types of RRP wires in terms of position, volume, orientation, and dimensions. The following step will be the use of the data gained from the void analysis as statistical input for sophisticated finite element models to help predicting the electro-mechanical behavior of RRP wires and to identify solutions for improving their tolerance against stress.

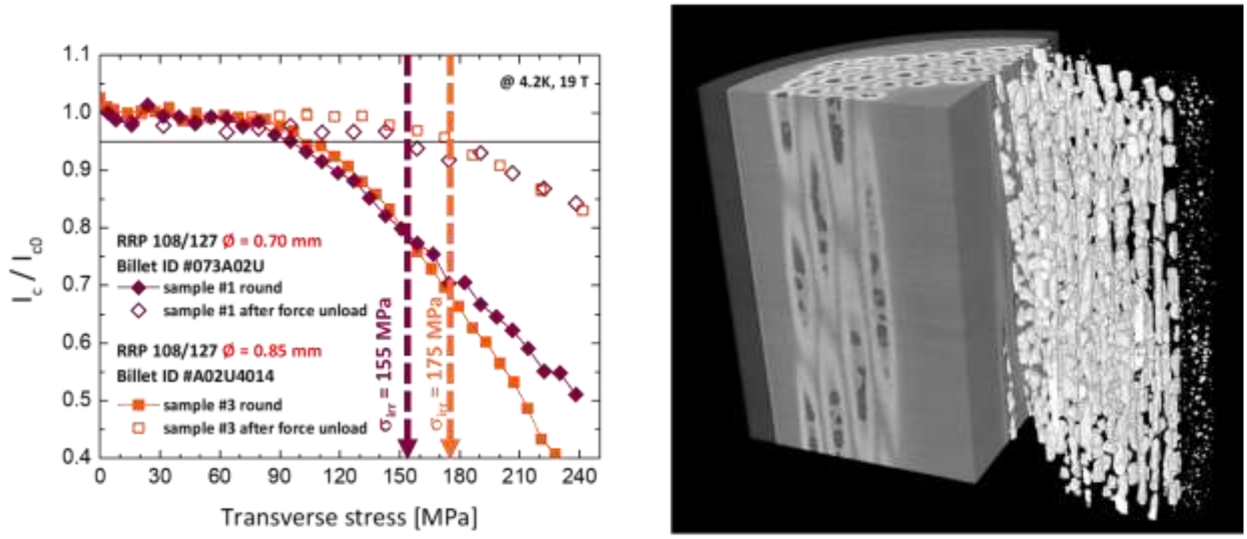

Figure 2.2 (Left) Dependence on the applied transverse stress at *T* = 4.2 K, *B* = 19 T of the critical current I_c normalized to the critical current at zero applied stress, I_{c0}, for the RRP 108/127 wires at 0.85 mm (squares) and at 0.7 mm (diamonds). Solid and open symbols correspond to the measurement under load and after unload, respectively. Dashed lines indicate the irreversible stress limits. (Right) X-ray tomography volume reconstruction and voids detection of an RRP 108/127 wire.

References

[1] D. Tommasini, et al., "The 16 T Dipole Development Program for FCC," *IEEE Trans. Appl. Supercond.*, vol. 27, 6600705, 2017.

[2] P. J. Lee, and D. C. Larbalestier, "Microstructure, microchemistry and the development of very high Nb_3Sn layer critical current density," *IEEE Trans. Appl. Supercond.,* vol. 15, pp. 3474-3477, 2005.

[3] X. C. Xu, "A review and prospects for Nb_3Sn superconductor development," *Supercond. Sci. Technol.,* vol. 30, p. 093001, 2017.

[4] X. Xu, et al., "Refinement of Nb_3Sn grain size by the generation of ZrO_2 precipitates in Nb_3Sn wires," *Appl. Phys. Lett.,* vol. 104, p. 082602, 2014.

[5] F. Buta, M. Bonura, D. Matera, G. Bovone, A. Ballarino, S. C. Hopkins, B. Bordini, X. Chaud, C. Senatore, "Nb_3Sn superconductors with internally oxidized Zr and Ta doping: Superconducting properties and microstructure," submitted to *Supercond. Sci. Technol.*

[6] L. Gämperle, J .Ferradas, C. Barth, B. Bordini, D. Tommasini, C. Senatore, "Determination of the electromechanical limits of high-performance Nb_3Sn Rutherford cables under transverse stress from a single-wire experiment," Phys. Rev. Research., vol. 2, p. 013211, 2020.

[7] J. Ferradas Troitino, T. Bagni, C. Barth, B. Bordini, P. Ferracin, L. Gamperle, D. Tommasini, D. Zurmuehle, C. Senatore, "Effects of the initial axial strain state on the response to transverse stress of high-performance RRP Nb_3Sn wires," submitted to *Supercond. Sci. Technol.*

[8] T. Bagni, G. Bovone, A. Rack, D. Mauro, C. Barth, D. Matera, F. Buta, C. Senatore, "Voids in RRP Nb_3Sn wire and their implications on electro-mechanical and electrothermal stability: an X-ray tomography analysis," submitted to *Sci. Reports*

3. Report on MagAM (Additive Manufacturing for Structural Components in Superconducting Coils) activities at ETHZ

Patrick BEUTLER, Christoph KLAHN
ETHZ pd|z and Inspire AG

This report is divided into two parts. The first part summarizes the findings of a pilot study, which was conducted between Summer 2019 and Spring 2020. Based on this pilot study a CHART project called MagAM was initiated and started in Mai 2020. The second part of the report gives insights to ongoing work and preliminary results of the MagAM project.

3.1 Pilot Study – Manufacturability Proof and Pre-Study on Adhesive Joints

The canted cosine theta (CCT) technology, which is investigated at PSI, leads to very complex metal structures for the coil geometry. Since these structures are difficult to manufacture with subtractive manufacturing methods, other manufacturing technologies like Laser Powder Bed Fusion (L-PBF) should be considered. While L-PBF enables the production of complex geometries, the manufacturing of overhang structures is restricted to avoid dross formation, cracks in overhang surfaces and reduce thermal warpage. The CCT coil geometry consists of some critical overhang structures that are not able to be manufactured with standard process parameter sets. The aim of the pilot study was to manufacture extreme overhangs with functional surfaces. Therefore, a parameter model was developed and the coil was successfully manufactured. This highlights the potential of Metal Additive Manufacturing for the coil production. In the pilot study, the following results were achieved:

- The parameter model investigated simplified geometries combined with a variety of L-PBF process parameter sets and different overhang angles. The model shows a dependence between L-PBF process parameters (e.g. laser power, scan speed) and the critical overhang angle. A section of a CCT coil has successfully been manufactured from stainless steel 316L (Figure 3.1 right). The part was divided into multiple segments (Figure 3.1 left) and the segments were assigned specific process parameter sets. This approach yields to better geometrical accuracy, better surface roughness properties and locally adjustable material properties.

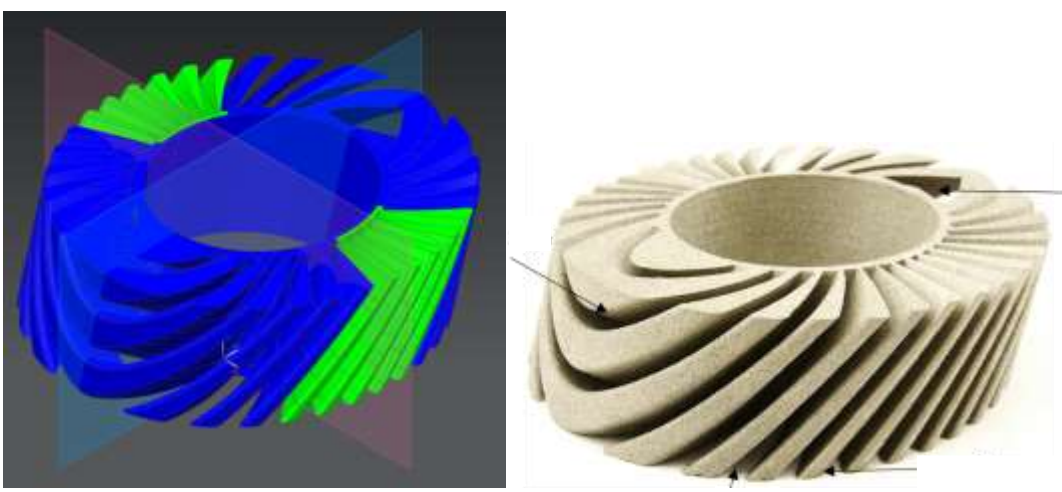

Figure 3.1 Left: Segmented part where the color indicates the assigned set of process parameters. Right: Final part of L-PBF manufactured CCT coil section.

- A second study on the improvement of the adhesive properties between the steel coil and the epoxy impregnated cable windings was conducted during the pilot study. In this scope four different surface structures were investigated (see Figure 3.2) and the ultimate strength of their adhesive joint was tested in a compressive shear test. The results of the shear test has shown that samples with surface texturing (see Figure 3.2, Design b) lead to significantly higher maximum shear strength compared to non-structured L-PBF samples and compared to conventionally manufactured samples (Ferchow, et al., under peer review, 2021).

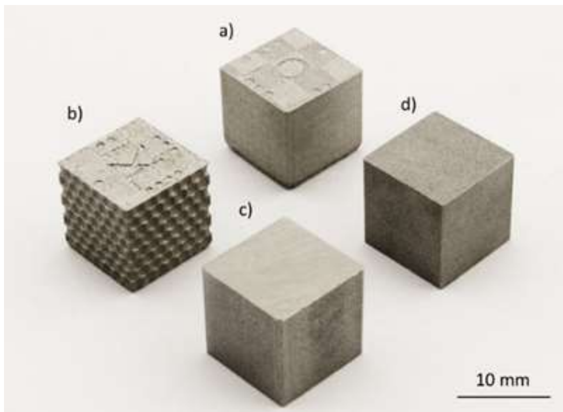

Figure 3.2 Left: Surface structures: a) L-PBF flat surface, b) L-PBF textured surface, c) Blank steel, d) Blank steel corundum blasted. Right: Test setup for compressive shear test

One master thesis (Müller, 2020) and one journal publication (Ferchow, et al., Under Blind Peer Review, 2021) (not published yet) have resulted from the pilot study.

3.2 MagAM

An explorative study on the effect of surface structures on the ultimate strength of adhesive joints was designed based on the promising results of the pilot study. The designs include triply periodic minimal surface (TPMS, Gyroid) structures, lattice structures (octet without horizontals) and structures with surface textures (sinusoidal dimples, undercut). The idea behind lattice and TPMS structures is to create an interpenetrating phase layer (IPL) where both epoxy and metal are present and thus a smooth transition between their mechanical properties in the dissimilar material joint is achieved. The adhesive joints are going to be tested under tension and shear loads. The tests are both conducted at ambient and cryogenic temperature (liquid N2).

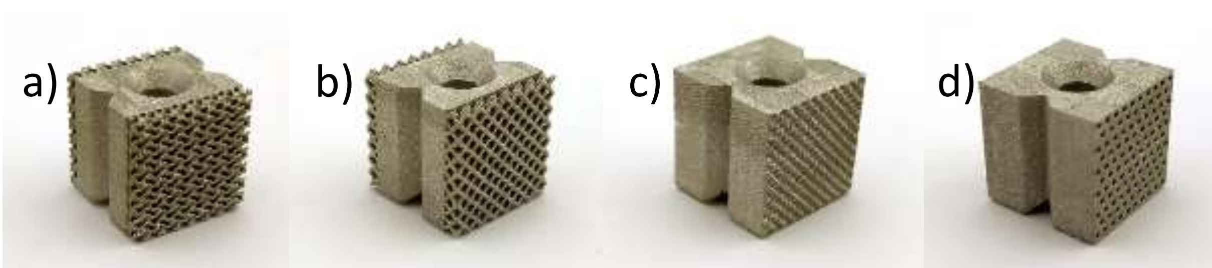

Figure 3.3 Compressive shear sample designs for the explorative study: a) TPMS Gyroid structure, b) Lattice Octet w/o horizontals structure, c) sinusoidal simple structure, d) Undercut structure

The optimization of the impregnation process of testing samples with the epoxy system is currently investigated. A mold design has been developed to repeatably place the samples with a defined adhesive gap and orientation to each other. Further, a lab scale impregnation process was developed to impregnate the samples under vacuum with the epoxy to avoid air bubbles. To measure the quality of this process a collaboration was started with Professor Schütz at HSLU to analyse the amount and distribution of air bubbles under a CT-scan. Preliminary shear tests with the shear sample design lattice (octet w/o horizontals) lead to ultimate strength values of up to 23MPa at ambient temperature and up to 40MPa in liquid nitrogen.
The next steps are to conduct the test series and further investigate the most promising designs. To do so, a surface structure will be applied to a small scale winding prototype in collaboration with PSI. At the same time the experimental results should be used as validation to build a FEM simulation for adhesive joints. Two master thesis are currently conducted at ETH Zürich. The first master thesis works on the impregnation process and the second on the FEM simulation of adhesive joints.

MagAM Team

A comprehensive list of team members in the past year of the project is reported below.

Person	Function	Period	Percentage	Funding
Christoph Klahn	PostDoc	May 20 - Nov 20	8%	CHART
Patrick Beutler	PhD	May 20 - Nov 20	100%	CHART
Philip Dalla Palma	Master thesis	Aug 20 - Feb 21	100%	n/a
Tiago Ogris	Master thesis	Okt 10 - Apr 21	100%	n/a

Publications

Ferchow, J., Biedermann, M., Müller, P., Auchmann, B., Brem, A., & Meboldt, M. (Under Blind Peer Review, 2021). Opportunities and Fundamental Challenges of Part Segmentation in Metal Additive Manufacturing - A Case Study on a Superconducting Solenoid Coil.

Müller, P. (2020). Master Thesis - Enabling Complex SLM Parts Based on a Process Parameter Model. *ETH Zürich - Product Development Group pd|z.*

4. Progress Report on ETH Zurich-SMG MagRes activities

André BREM, Pascal STUDER and Theo TERVOORT
ETHZ D-MATL, SMG

Introduction

The ETHZ-SMG CHART2 project MagRes has started in September 2020 with a new PhD student, Pascal Studer, who was trained on the job by André Brem, the post doc carrying out resin CHART1 R&D. In CHART1, various characterization methods at cryogenic (liquid nitrogen) temperatures have been developed and applied to selected epoxy systems. The bulk of experimental results and insights has been published in [1]. The effort of CHART1 will continue in CHART2 and will be extended to include the determination of other properties of interest, the study of new materials, and the comprehensive constitutive models for FEA simulations. Below we summarize the CHART2 MagRes results acquired so far:

Compression Testing

In order to characterize the plastic deformation of various epoxy systems at cryogenic temperatures, uniaxial compression testing will be performed, both under liquid nitrogen (LN), and liquid helium (LH) conditions. If possible, mechanical testing will be performed as a function of strain rate and temperature. For the results described in this report, all testing was performed on a Zwick Z202 tensile tester equipped with a 20 kN load cell. To avoid any friction between the sample surfaces and the compression plates, a thin film of PTFE oil was spread on the compression plates.

Long-term loading conditions

As the epoxy systems will be submitted to long-term loading conditions, it will be of interest to measure the relaxation behavior under cryogenic temperatures and at room temperature. For the results in this report, relaxation measurements were performed on a TA Instruments Ares G2 in combination with a forced convection oven.

4.1. Compression Testing of Loctite Stycast

Loctite Stycast is a highly filled, thermally conductive epoxy system recommended for encapsulation of components that require heat dissipation and thermal shock properties and that is often used in magnet applications.

Cylindrical samples of 8 mm diameter and 8 mm height were subjected to uniaxial compression testing with a constant velocity, corresponding to initial strain rates of 10^{-3}, 10^{-2} and 10^{-1} s^{-1}. The measured yield stresses as a function of strain rate are depicted in Figure . The yield stress of the Stycast epoxy appears to follow the Eyring theory. The Eyring theory states that the yield stress is a function of applied strain rate as[2]:

$$\sigma_y = \tau_0\sqrt{3}\ln\left(2\sqrt{3}\right) + \tau_0\sqrt{3}\ln\left(\frac{\dot{\varepsilon}}{\dot{\gamma_0}}\right) \tag{1}$$

Here, τ_0 and $\dot{\gamma}_0$ are material parameters. According to the Eyring theory, a semi-log plot of the yield stress as a function of strain rate should result in a straight line. This was indeed the case as can be seen in Figure . The best fit resulted in values of τ_0 = 3.3 MPa and $\dot{\gamma}_0 = 2.5 \times 10^{-10}\ \mathrm{s}^{-1}$. In the near future, the yield stress of Stycast at cryogenic temperatures will be evaluated.

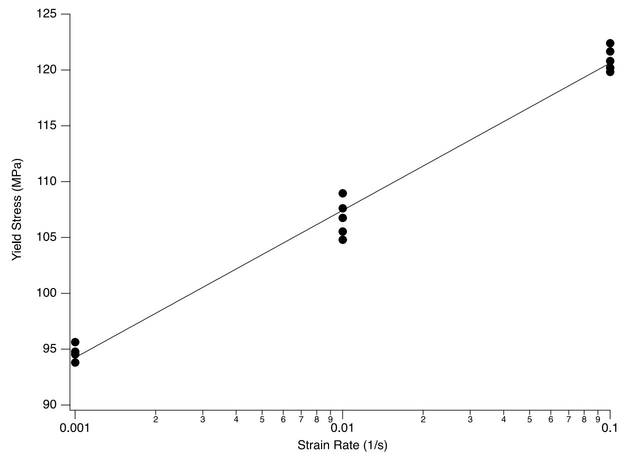

Figure 4.1: Yield stress of Stycast as a function of strain rate. The dots are experimental values, and the solid line is the best fit using the Eyring theory.

4.2 Relaxation behavior of CTD 101K, Mix61 and MY750

According to linear viscoelastic theory[3], creep and relaxation behavior can all be described by the relaxation modulus $E(t)$, which describes the mechanical response of a material following a unit step in strain. The relaxation modulus was measured for three epoxy systems: CTD101K, Mix61 and MY750. To avoid excessively long measuring times, time-temperature superposition was used to access the relaxation behavior at long times. This is achieved by measuring the relaxation modulus at different temperatures and shifting the curves along the logarithmic time axis to build a master curve. The original measurements and the master curves at 30 °C are shown in Figure -Figure.4. From these figures it is clear that at 30 °C, large differences exist between the relaxation behavior of these epoxy systems. For example, at 30 °C, after 30 days (2.6×10^6 s), CTD101K relaxes "only" 20% of the initial stress, while MY750 and Mix61 relax the initial stress for 88% and 85%, respectively. This is most probably due to the near proximity of the glass transition temperature at 30 °C for the latter two epoxy systems. In the near future, the relaxation behavior at LN temperatures will be evaluated. In addition, it will be attempted to describe and evaluate the non-linear stress relaxation at finite deformations and high stress levels.

From a magnet-builder's perspective, these results are of paramount importance. While Mix61 and MY750 have the advantage of high fracture toughness and low thermal load after cool-down, the latter owing to the lower glass-transition temperature, the pronounced relaxation effect at room temperature may well disqualify them for use in a mechanically pre-loaded magnet concept like the current cosine-theta and block-coil designs of the FCC Conceptual Design Report. Alternative routes will be studied to "toughen" existing materials like CTD101K with nano fillers, without impacting their high glass transition temperature and long relaxation time constant.

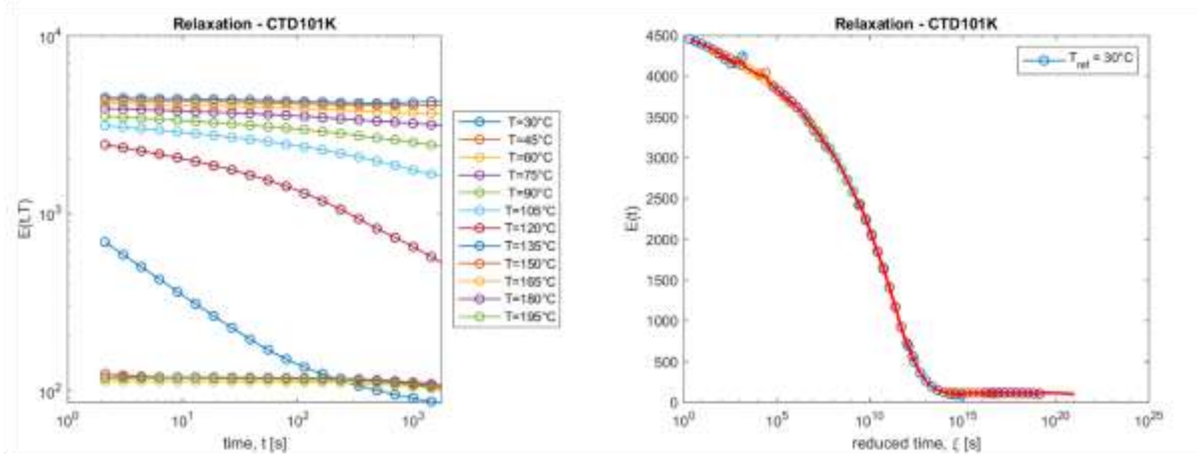

Figure 4.2: Relaxation modulus of CTD101K measured at different temperatures (left) and the resulting mastercurve at a reference temperature of 30 °C.

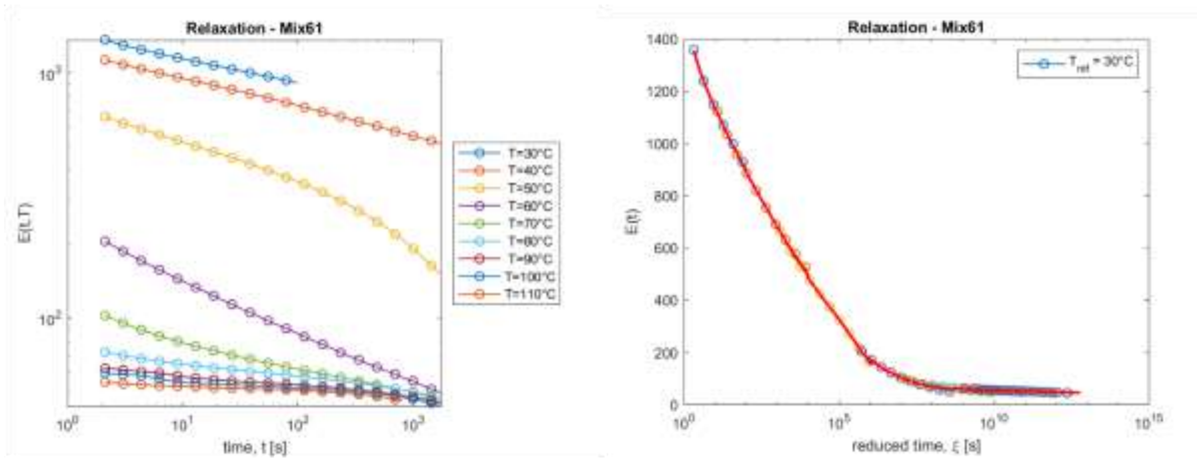

Figure 4.3: Relaxation modulus of Mix61 measured at different temperatures (left) and the resulting mastercurve at a reference temperature of 30 °C.

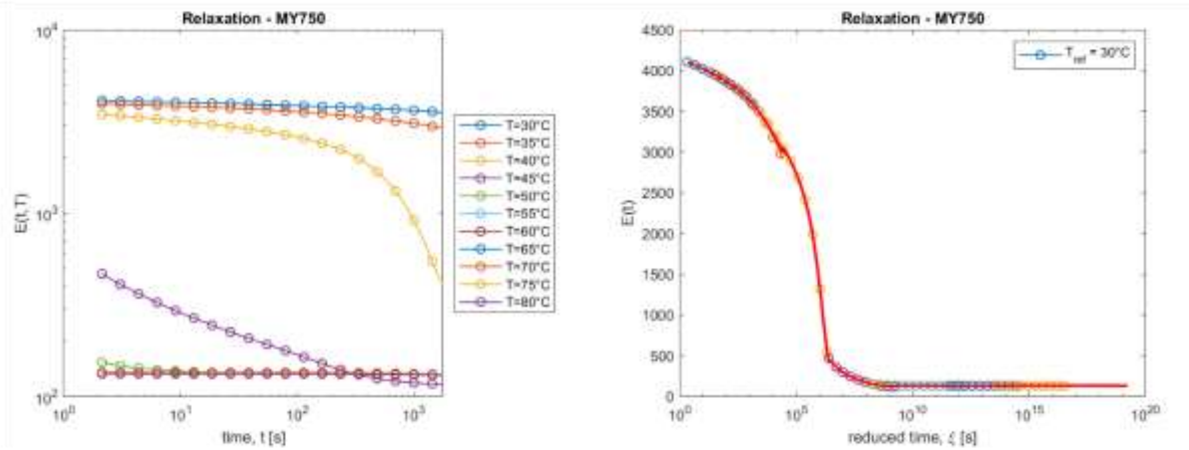

Figure 4.4: Relaxation modulus of MY750 measured at different temperatures (left) and the resulting mastercurve at a reference temperature of 30 °C.

References

[1] Brem, A.; Gold, B.; Auchmann, B.; Tommasini, D.; Tervoort, T. A. Elasticity, Plasticity and Fracture Toughness at Ambient and Cryogenic Temperatures of Epoxy Systems Used for the Impregnation of High-Field Superconducting Magnets. *Cryogenics, Accepted,* **2021**.

[2] Eyring, H. Viscosity, Plasticity, and Diffusion as Examples of Absolute Reaction Rates. *J. Chem. Phys.* **1936**, *4* (4), 283–291. https://doi.org/10.1063/1.1749836.

[3] Ferry, J. D. *Viscoelastic Properties of Polymers*; Wiley: New York, 1980.

5. Report on Beam Dynamics activities at EPFL

Tatiana Pieloni, EPFL

The beam dynamics studies have been focused on three different topics:

- Continue and extend the **instability, Landau damping and emittance evolution studies** related to FCC via simulations. In addition, full analyses of data from the LHC available from the RUN2 dedicated experiments have been conducted.
- Develop a new correction scheme for the LHC experiments evaluation of the **absolute luminosity determination with beam-beam effects** during Van der Meer (VdM) scans analysis
- **Machine Learning exploration** for possible use in future colliders design or for further exploitation of LHC data or operation time.

5.1 Beam Stability

The study of beam stability and preservation of beam parameters have been conducted for the FCC hadron colliders and studies have been described in the extended version of the Conceptual Design Report for FCC-hh. The main results have been summarized and used to define the operational scenario for the hadron colliders to reach the luminosity goals. Studies have been carried in static considerations without considering dynamic changes of parameters as emittance and intensities of the beams. The effects analyzed with the proposed scenarios are summarized in [1] and [2] for the baseline choice. In addition results have been published in [3][4][5].

In parallel during the last year we have focused on comparing existing models used for FCC-hh design with LHC data to verify the validity of such models. A full analysis of the available data from dedicated machine experiments on the LHC during RUN2 has been carried out and documented in [6][7][8]. The studies where covering the modification of the stability thresholds when an impedance is presence and in the presence of an external noise source as for example the transverse feedbacks used to suppress dipolar oscillations.

The presence of a diffusive mechanism has shown to be detrimental for Landau damping and therefore in the design one should account for keeping these effects under defined threshold dictated by stability. This means tighter tolerances for element vibrations in general respect to the LHC. The tolerances should be revised and impact to stability should be re-evaluated. This is evident in the experimental and numerical prove of the deviation of the stability thresholds when diffusion is present as described in [9]. In Figure 5.1 the stable phase scale which represent the stability expectation is shown from models (solid line) and from LHC measurements. A deviation from models reducing the stability if visible for the Vertical plane (red line) and this can be correlated to a faster diffusion in the vertical plane as shown in Figure 5.2. The development of the Beam Transfer Function measurements [10][11][12][13][14] have opened the possibility to explore experimentally the Landau damping properties of the beams and more recently also to possibly use such device for a parasitic measurements of chromaticity. In addition the effect of the transverse impedance and chromaticity on the BTF measurements have highlighted a factor 1.5 stronger impedance in the LHC [7].

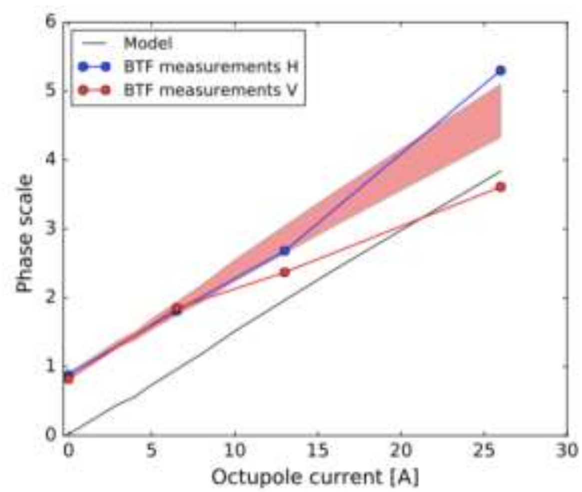

Figure 5.1 The phase scale parameter evaluated from the fitting function applied to the BTF measurements at injection energy as a function of the octupole current. The blue dots represent the BTF measurements in the horizontal plane, and the red dots are the measurements in the vertical plane. The solid black line represent the expectations from the model with respect to a which no asymmetry in the two transverse planes has been observed and for direct comparison with the operational octupole settings at the time of the measurements. As expected for such a current, the phase scale of the model is equal to one. The red shadow is given by the model expectations including the initial nonzero tune spread corresponding to ≈5.5 A and considering an uncertainty of 10% on the measured emittance.

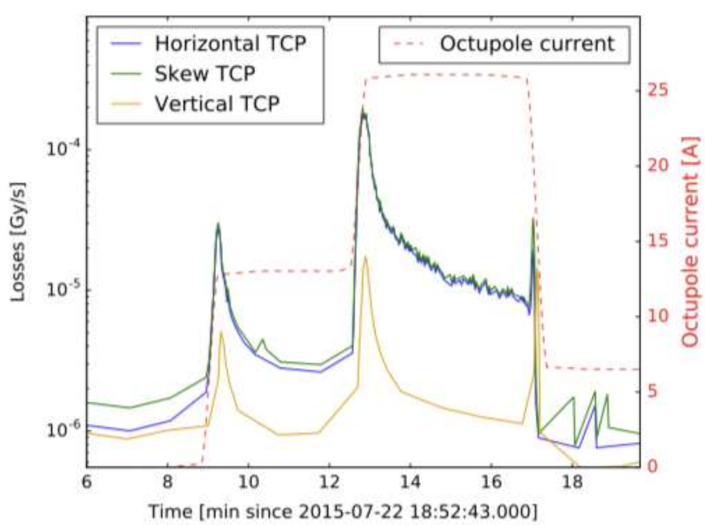

Figure 5.2 Particle losses detected by the Beam Loss Monitors (BLMs) at the primary collimators location in IR7 as a function of time while changing the octupole current (the dashed red line).

The present understanding of the emittance growth rate of colliding beam due to decoherence in the LHC can be described with a numerical model based on macroparticle tracking simulations. The models well describe the observed emittances qualitatively but can give a realistic numerical comparison when an external source of noise is introduced. Present models can be used for extrapolation to future machine. The experiments revealed a significant contribution of the existing transverse feedback to the emittance growth driven by its BPM noise floor, such that mitigations might be required to achieve the performances goals. The other sources of noise in the LHC remains to be identified and therefore will require further studies during RUN3. All the findings will have to be translated in terms of tolerances for the FCC-hh and HE-LHC design. The full analysis can be found in [15] with estimates for the HL-LHC. With these findings in mind a study on the possible impact on noise due to an electron lens has started and a clear impact is visible [16]. The side effects of such element should be analysed from the stability point of view also in view of a possible use of such devices in the HL-LHC.

5.2 Absolute Luminosity and beam-beam effect

LHC experiments need the evaluation of the absolute luminosity to be able to calibrate their detectors. This calibration occurs during dedicated experiments in the LHC and uses the well-established Van der Meer (VdM) methodology. In 2019 it has been shown that the collective effect known as beam-beam interaction does contribute to the luminosity determination when the VdM method is used. In this frame we have developed the numerical tools to be used to determine luminosity during a VdM scan and to account for the beam-beam effects (all developed in the COMBI code) [17]. A full parameter and sensitivity studies campaign has been carried out to provide the four LHC experiments (ATLAS, CMS, LHCb and Alice) with a common correction scheme to be applied in their luminosity analysis. Results and the correction strategy will be published in [18] for the VdM cases. In Figure 5.3 the luminosity ratio is shown as a function of the beam to beam separation during a typical van der Meer scan. In the figure we compare the ratio using the old linear correction (blue line), when a correct beam-beam beating is accounted for (red line) and if the luminosity is computed by the overlap integral without assuming a Gaussian distribution for the particles. Further studies will follow to address the impact of beam-beam interactions in the presence of bunch train configurations and crossing angles as in operational mode.

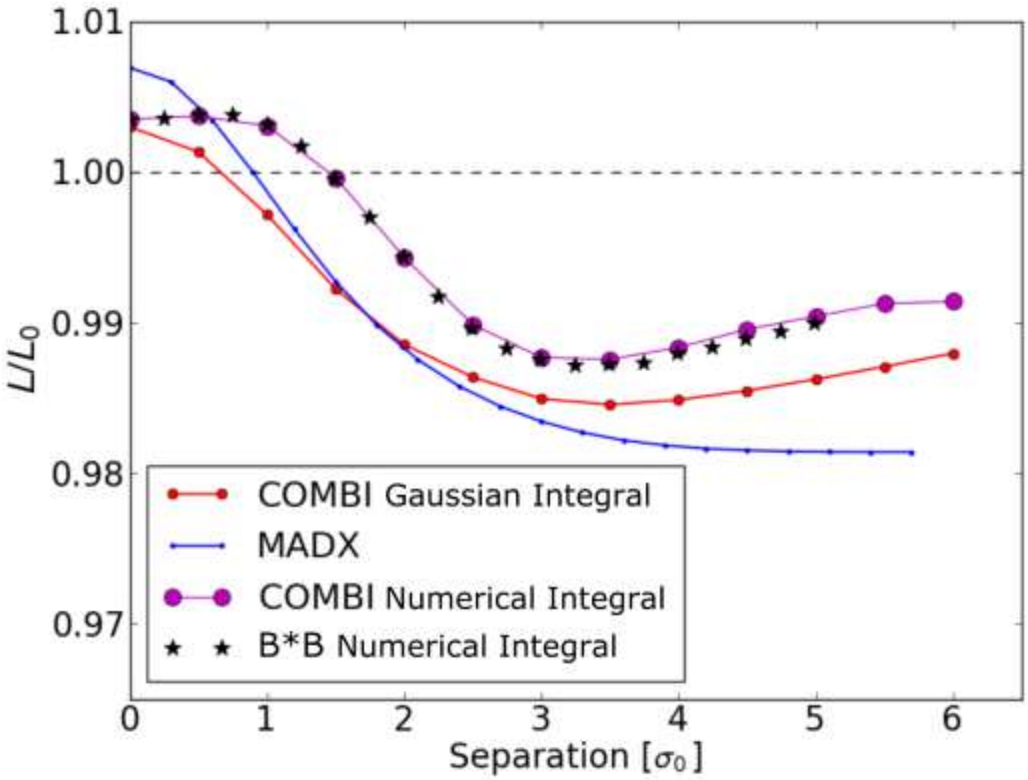

Figure 5.3. Luminosity ratio between computed luminosity without beam-beam effect L0 and the results of multi-particle effects L for different relative beam to beam separations during a typical Van der Meer scan expressed in units of the transverse RMS beam size 0 for the different models used.

5.3 Machine Learning

Another important path that is under exploration is the possibility to use modern Machine Learning (ML) and artificial intelligence technologies to the design and operation of colliders. These studies are done in collaboration with the SDSC and the LHC operation group at CERN. In this frame we have explored three possible applications:

- Beam lifetime optimization for the LHC
- Instability detection using the ADT ObsBox for online fast data analysis and instability classification for RUN3
- Anomaly detection of anomaly beam loss maps from RUN2 LHC data and possible implementation for RUN3

The first two topics have been described in a common paper [19]. In Figure 5.4 an example of the comparison of a machine learning optimized working point (red dot) versus the machine operational working point (blue dot) and data acquired during a dedicated experiment in the LHC during RUN2 (yellow dots have higher beam lifetime). The new optima seems showing a better operational set-up with much larger lifetimes.

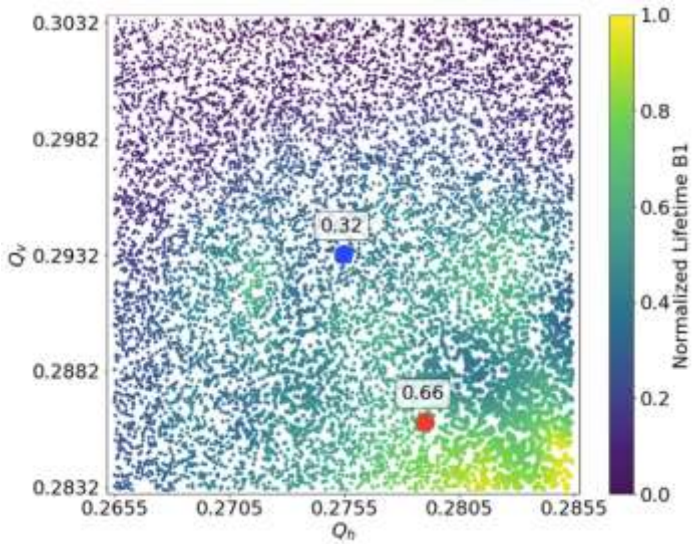

Figure 5.4 Normalised beam lifetime as a function of the LHC tune working point as measured for Beam 1. Blue dot: Nominal working point. Red dot: Lifetime-optimised working point as determined by the ML model. The model prediction is close, but not exactly equal, to the measured maximum lifetime. The absolute minimum and maximum value of the beam lifetime is 1.05 h and 32.7 h, respectively.

Publications:

1. Future Circular Collider Study. Volume 3: The Hadron Collider (FCC-hh) Conceptual Design Report, preprint edited by M. Benedikt et al. CERN accelerator reports, CERN-ACC-2018-0058, Geneva, December 2018. Published in Eur. Phys. J. ST.
2. Future Circular Collider Study. Volume 4: The High Energy LHC (HE-LHC) Conceptual Design Report, preprint edited by F. Zimmermann et al. CERN accelerator reports, CERN-ACC-2018-0059, Geneva, December 2018. Published in Eur. Phys. J. ST.
3. Jose L. Abelleira et al., FCC-hh Experimental Insertion Region Design, https://arxiv.org/abs/2007.12058
4. L. van Riesen-Haupt *et al.*, "Developments in the Experimental Interaction Regions of the High Energy LHC", in *Proc. IPAC'19*, Melbourne, Australia, May 2019, pp. 532-535. doi:10.18429/JACoW-IPAC2019-MOPMP039
5. F. Zimmermann *et al.*, "Updated High-Energy LHC Design", in *Proc. IPAC'19*, Melbourne, Australia, May 2019, pp. 524-527. doi:10.18429/JACoW-IPAC2019-MOPMP037
6. C. Tambasco et al., MD 3292: MEASUREMENTS OF LANDAU DAMPING BY MEANS OF BTF MEASUREMENTS, Machine Development Report, CERN-ACC-Note-2019-0045.
7. C. Tambasco et al., MD 3290: Instability threshold measurements in the presence of a controlled external excitation, Machine Development Report, CERN-ACC-Note-2019-0044.
8. S. V. Furuseth et al., MD3288: Instability latency with controlled noise, CERN-ACC-NOTE-2019-0011.
9. C. Tambasco et al., "Beam transfer function measurements used to probe the transverse Landau damping at the LHC", Phys. Rev. Accel. Beams, vol. 23, no. 071002, 2020, doi: 10.1103/PhysRevAccelBeams.23.071002

10. C. Tambasco *et al.*, “Beam Transfer Function Measurements and Transverse Stability in presence of Beam-Beam”, *in ICFA Mini-Workshop on Impedances and Beam Instabilities in particle accelerators*, Benevento, Italy, *pp.105-109*, doi: 10.23732/CYRCP-2018-001.105
11. C. Tambasco *et al.*, “Landau Damping Studies for the FCC: Octupole Magnets, Electron Lens and Beam-Beam Effects”, in *Proc. 9th Int. Particle Accelerator Conf. (IPAC'18)*, Vancouver, BC, Canada, Apr. 4, pp. 3150-3153, doi:10.18429/ JACoW-IPAC2018-THPAF074
12. ICFA mini-workshop on Mitigation of Coherent Beam Instabilities in particle accelerators (MCBI 2019), *BTF and stability diagram*, C. Tambasco, Zermatt, Switzerland, September 2019
13. ICFA mini-workshop on Mitigation of Coherent Beam Instabilities in particle accelerators (MCBI 2019), Review of instabilities with beam-beam and possible mitigations, T. Pieloni, Zermatt, Switzerland, September 2019.
14. ARIES-APEC workshop on Mitigation Approaches for Hadron Storage Rings and Synchrotrons, Injecting ripples on beam: shall we?, C. Tambasco, June 2020
15. X. Buffat, W. Herr, T. Pieloni, and D. Valuch, Modeling of the emittance growth due to decoherence in collision at the Large Hadron Collider, Phys. Rev. Accel. Beams 23, 021002 – Published 18 February 2020
16. R. Cai et al., Simulations of particle loss due to hollow e-lens and non-linearities for the HL-LHC, CERN-ACC-NOTE-2020-0046.
17. T. Pieloni and C. Tambasco, Beam-beam simulations with COMBI & TRAIN in vdM fills, Lumi days 2019. Lumi talk.
18. A. Babaev et al., Impact of Beam-Beam Effects on Absolute Luminosity Calibrations at the CERN Large Hadron Collider, to be published.
19. P. Arpaia, G. Azzopardi, F. Blanc, G. Bregliozzi, X. Buffat, L. Coyle, E. Fol, F. Giordano, M. Giovannozzi, T. Pieloni, R. Prevete, S. Redaelli, B. Salvachua, B. Salvant, M. Schenk, M. Solfaroli Camillocci, R. Tomás, G. Valentino, F.F. Van der Veken, J. Wenninger, Machine learning for beam dynamics studies at the CERN Large Hadron Collider, Nuclear Instruments and Methods in Physics Research Section A: Accelerators, Spectrometers, Detectors and Associated Equipment, Volume 985, 2021,164652, ISSN 0168-9002.

6. Report on High Brightness HTS Undulators (HTSU) activities at PSI

M.Calvi[1], S. Hellmann[1], R. Kinjo[2], X. Liang[1], K. Zhang[1].

[1] Photon Science Division, Paul Scherrer institut, Switzerland ;

[2] RIKEN SPring-8 Center, 1-1-1 Kouto, Sayo-cho, Hyogo 679-5148 Japan ;

This project has the ambition to demonstrate a new undulator technology for achieving a much higher brightness than the state-of-the-art spell CPMUs[1]. It has the potential to push the world community of synchrotron radiation sources to equip the hard X-Ray beamlines of the new Diffraction Limited Storage Rings and future Compact FELs [1] with this new technology, as it was the case for in-vacuum undulators in the past. The success of this prototype will require a technology transfer to profit from the expected favourable business case. HTSUs will not only improve and speed up existing activities at the beamlines but they will allow new experiments in medium energy storage rings today possible only in the few large existing facilities, like APS, SPring-8 and ESRF.

A high-profile application example is undulator-based tomography [5] of high-Z material with dimensions of the order of a few millimetres, where high photon energies and high flux density are required to get through samples of the same order of magnitude linear dimensions. In addition, phase-contrast tomography is required for fast tomography in the 10-100 Hz tomogram rate, which can only be provided by the relatively high coherent fraction offered by undulators.

In the following, the summary of the project status is presented divided in five sections covering the main projects activities and ending with an overview of the project management and collaborations.

6.1 Simulation design studies

The specific design of the superconducting staggered array undulator requires simulation studies on the magnetisation of the individual HTS blocks. This issue has been tackled in a first attempt with the H-formulation of the Maxwell equations and the commercially available code COMSOL Multiphysics®. This approach has been implemented in collaboration with simulation experts of Karlsruhe Institute of Technology, F. Grilli and co-workers. This method, very well understood and applied successfully to many technical problems, has been used in the field of undulators for the first time [6], with the aim of optimising its performances and better understanding its limits, see Figure 6.1. New geometries have been proposed and analysed for the first time, including a field enhanced version making use of iron poles and a circular polarised field distribution with a segmented helical geometry.

The baseline option of the project is the Rare Earth Barium Copper Oxide (ReBCO) bulk material, at this time the technology with the highest engineering current density. An alternative solution with ReBCO tapes has been proposed and simulated. The field performance is 30% lower but they might be finally chosen if the regular bulk option would not meet the requirements in terms of homogeneity of the crystal and reproducibility of the manufacturing processes. Additionally, tapes are mechanically stable thanks to the Astaloy (or Stainless Steel) substrate whereas bulk blocks have to be reinforced and pre-stressed with additional structural elements.

---

[1] Cryogenics Permanent Magnet Undulators.

After a preliminary learning period using the H-formulation and COMSOL multi-physics, we proposed new approaches implemented in ANSYS. The first makes use of an iterative algorithm and both the critical state model and the flux creep model have been implemented [7]. The second method is computationally very efficient and is based on the backwards calculation of the critical state model. Indeed, it starts from the eddy current estimation using the A-V method and the algorithm relaxes the solution to comply with the constrains given by the finite critical current density Jc(B,T) value [8]. These approaches have been compared with the baseline H formulation, both in terms of accuracy and computational efficiency. Most recently, the equivalence of the backward computation method to other numerical methods, namely the Minimum Electro-Magnetic Entropy Production (MEMEP) method [9] and the field-screened method [10], is validated. This new backwards calculation has been further extended to compute the critical state currents in 3D bulk HTS undulator, showing highly efficient computation on large-scale modelling with over 10 million degrees of freedom (DOFs). The related paper is under preparation.

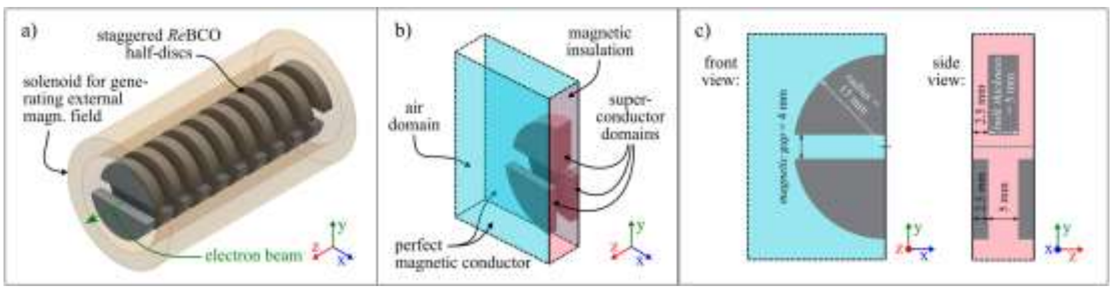

Figure 6.1 (a) Full geometry of a ten-period staggered array undulator consisting of 20 ReBCO half discs. In the application as an undulator in an electron accelerator the electron beam travels between the upper and the lower row of ReBCO bulks. (b) Simulation model using two symmetries in the model. These are implemented by a magnetic insulation and perfect magnetic conductor boundary conditions. (c) Dimensions of the reference undulator geometry and optimisation parameters radius, bulk thickness and magnetic gap (the depicted sketches are not to scale).

The models have been used also to optimise the end field for matching the first and second field integrals, to analyse the experimental data (evaluation of the Jc from the field distribution) and to develop a "shimming" strategy. On the latter, a new approach is under development which consists of a local variation of the period to compensate the deviation of the peak magnetic field from the target value. This publication is under preparation, highlighting the advantages of this approach compared and associated with more conventional ones.

To conclude this section about simulation design study, we would like to remind that superconducting undulators up to now have been manufactured with coil windings and their field optimisation is still an open issue. This approach is the superconducting version of permanent magnets (they are also called superconducting permanent magnets) and allow to profit from many techniques developed during the last 30 years in that domain.

6.2 Short Sample Tests

This experimental activity consists of the cold test of undulator samples made of 10 periods (about 10 cm long). As a project strategic decision, this activity was planned to be carried out in collaboration with the Bulk Superconducting Group of the University of Cambridge, making use to their experience and test stations. Two campaigns were carried out on samples of different geometries and tested in different conditions, like temperature and ramp-rate. The samples were prepared with ReBCO crystals (melt textured) produced, machined and assembled at the University. The first sample had the nominal period length and bulk diameter respectively of 10 mm and 30 mm and the magnetic gap of 6.0 mm (larger than the nominal 4.0 mm to speed up the first testing phase when only a probe of 4 mm was originally available). The details of that measurement campaign are available in [11], where the results are presented and compared with simulations. Performance limitations were observed due to the sudden quench of the sample close to an on-axis undulator field of 0.85T. They were supposed to be generated by mechanical instabilities as on the one hand, the crystals were not permanently fixed into the copper matrix and on the other hand a small training (improving of the performances after repeating powering cycles) was observed. This interpretation was found to be most probably wrong since the reinforcement of the sample (the crystals were fixed with epoxy resin inside the copper matrix) had no impact on this phenomenon.

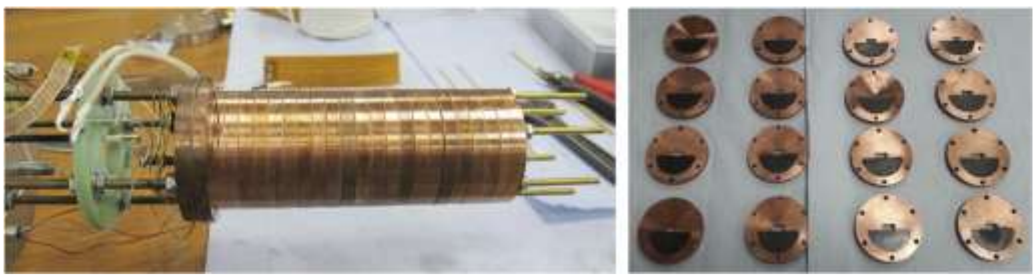

Figure 6.2 On the left a 10 cm long sample ready for testing, on the right the details of its components: the superconductor embedded into copper disk stabiliser and reinforced with epoxy resin impregnation techniques.

The second sample (Figure 6.2) was prepared with the nominal geometry thanks to a novel probe, which was developed meanwhile with compatible sizes for a gap of 4.0 mm. This sample was tested at 10 K and 20 K and the experimental results will be published shortly after completing the campaign. During this test a new reference undulator field of 1.3 T @ 10K was reached. During the campaign at 20K, it was possible to overcome the quench by lowering the ramp rate of the magnetisation coil (the external solenoid), from 4T/h to 1T/h, to reduce the losses.

Two new short samples were assembled and they will be tested during the first half of 2021. Differently than in the first two campaigns, these samples make use of industrial available superconductors and they are all assembled at PSI.

The first is made with GdBCO crystals (Ag reinforced) from CAN Superconductors, cut at the optimum shape by Laser MicroJet Technology and embedded into a copper matrix by thermal shrink-fit methods, see Figure 6.3. This procedure shall introduce enough pre-stress to allow for high field magnetisation, up to 12T trapped field. Together with the high manufacturing tolerances (<10 micron) achieved, this sample shall demonstrate the maximum field reachable and the intrinsic reproducibility of the crystal. If this attempt is successful, different material (YBCO, EuBCO, GdBCO) and different manufacturing (CAN, ATZ, NS) will be tested to compare their performance.

The second sample is made of ReBCO tapes, stacked in blocks of 100 and accurately cut with Wire Erosion. This approach is a solid (even if less performing) backup solution in case the reproducibility of the bulk production is demonstrated to be an obstacle to the required field quality. Because of the lower expected undulator field, this sample will be tested first in its enhanced version with iron poles which can be easily removed in a second attempt to have also a direct comparison with the bulk sample.

For both tests, a new measuring head with superior accuracy will be used. It was developed at PSI and delivered to the University of Cambridge in order to improve the positioning of the Hall probe sensor: both in the transversal plane by means of new set of cold Teflon guiding system anchored to an improved support and along the undulator axis (vertically) by means of a precise linear stage and encoder.

Figure 6.3 An example of industrial samples where the ReBCo bulks are machined with Laser Micro Jet and precisely assembled with in a copper matrix with shrink fitting techniques making use of high accuracy machining. Finally, the disks are stacked together and aligned using an external aluminum cylinder (in the above picture a cross-section is presented) to avoid relative displacement between the disks and to reach high geometrical tolerances in the final assembly (<10um).

6.3 Prototyping

The first meter long prototype will be installed into SLS 2.0 and serve the new microscopy tomography beamline, I-Tomcat. The backbone of this device is a 12T superconducting horizontal solenoid, 1.2 m long and with a cold bore of 100 mm diameter. This device is not readily available in industry both because of its size and field amplitude. For this reason, its design and assembly will be done in collaboration with Fermi National Accelerator Laboratory (FNAL) in USA. In Figure 6.4, a rendering picture of its cryostat is presented. We chose a conduction cooling scheme both for the solenoid and the HTS insert. The central cryocooler is connected to the solenoid while the two side ones are connected to the beginning and to the end of the insert.

6.4 Integration in the SLS 2.0

A preliminary study has been carried out to evaluate the compatibility of this undulator design with the beam dynamic of the storage ring. A background solenoidal field of up to 4T can be accepted only if its integral is cancelled with compensation coils and if the lattice is integrated with additional quadrupoles to account for focusing and coupling. One attractive solution would consist of two identical on axis solenoids with opposite signs, with an additional shifter in between to recover the phase when changing the undulator field. This solution would allow for an easy and fast selection of the radiated wavelength, changing the defection parameter as it is the case for conventional permanent magnet undulators. A simpler solution consists of a single solenoid operated at zero field after the magnetisation cycle. This device would not satisfy the requirement of a generic hard X-ray beamline but it fits the specification of a tomography beamline. Its reduced complexity and costs for the first test with beam makes it very attractive. This is the main reason why it was selected as the baseline for the I-Tomcat beamline of SLS 2.0.

6.5 Project Management & Collaborations

One of the two postdocs working on the project since May 2018, S. Hellmann, was hired by the PSI magnet section in May 2020 but he is still partially involved in our activities, especially in the final assembly of the new measuring bench and the future test of the tape-samples. The second postdoc working with us since October 2018, K. Zhang, got extended for the third year and in the meantime applied for an SNF AMBIZIONE grant. R. Kinjo, a scientist from **RIKEN Spring-8**, joined the project last fall. His salary is paid by his institute with a PSI contribution to make it compatible with standard PSI salary of the same level of expertise. He will stay at PSI until end of 2022 but we expect that an additional extension could be possible. On February 1st 2021, X. Liang joined the project as a PhD student of the **ETH Zurich**. He has been collaborating with us since spring 2019, in the domain of undulators as this milestone publication demonstrate [12]. His salary is financed by the **European grant, LEAPS-INNOV**. The access to the **University of Cambridge** facilities has been recently extended with an amendment to the collaboration agreement until 2022. The cost of the prototype superconducting solenoid to be built in collaboration with the US Department of Energy **Fermi National Accelerator Laboratory** (Fermilab) (cf. Fig. 6.4), estimated at 1.5 MCHF, will be covered by the budget of the SLS 2.0 project.

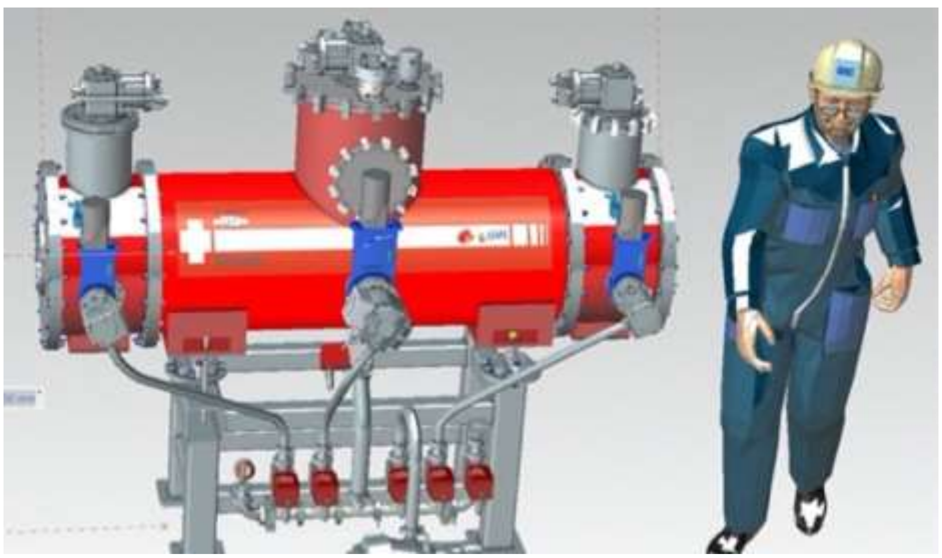

Figure 6.4. The design of the cryostat of the meter-long prototype done in collaboration with Fermilab. The cooling is based on conduction, powered by three cryocoolers: the central one dedicated to the superconducting solenoid and the two side ones dedicated to the HTS insert, the core of the undulator.

REFERENCES:

[1] XLS-Report-2019-004 27 June 2019 (https://www.compactlight.eu)

[2] Billinge S J L, Levin I 2007 Science 316 (5824), pp 561-565

[3] Chupas P J et al 2003 J. Appl. Cryst. 36, 1342-1347

[4] Bertolotti F et al 2016, Nature Materials 15, 987–994

[5] Stampanoni M et al CDR TOMCAT2.0: Multiscale Multimodal Dynamic Tomographic X-ray Microscopy, PSI Internal Document.

[6] Hellmann S et al 2020 IEEE Trans. Appl. Supercond. 30 (4) 4100705

[7] Zhang K et al 2021 IEEE Trans. Appl. Supercond. 31 (2) 20169576
[8] Zhang K et al 2020 Supercond. Sci. Technol. 33 114007
[9] Pardo E and Kapolka M 2017 J. comput. Phys. 344 339-63
[10] Coombs T A, Campbell A M, Murphy A and Emmens M 2001 COMPEL-The Int. J. Comput. Math. Electr. Electron. Eng. 20 240-52
[11] Calvi M et al 2020 Supercond. Sci. Technol. 33 014004
[12] Liang X et al 2021 NIMA 987 164741